Revealing the membrane fouling mechanism caused by the denitrification filter effluent during ozonation by model assessment

Yuan Bai, Yin-Hu Wu, Xin Tong, Yun-Hong Wang, Nozomu Ikuno, Wei Wang, Yu-Long Shi and Hong-Ying Hu IWA

ABSTRACT

Membrane fouling has been a major obstacle for stable operation of ultrafiltration. In this study, prevailing fouling models were applied to assess the fouling behavior of the denitrification filter (DNF) effluent during ozonation. In order to clarify the fouling mechanism, correlation analysis and redundancy analysis (RDA) were conducted to investigate the correlations among model parameters, fouling potential and water features of the DNF effluent. The combined intermediate-standard model exhibited superior determination coefficients ($R^2 > 0.99$). Based on analytical results, the model parameter of intermediate blocking (K_i) and standard blocking (K_s) was fairly applicable to describe the fouling of higher molecular weight (F1, MW $>$4,000 Da) and lower molecular weight fractions (F2, MW $=$ 2,000–4,000 Da and F3, MW $<$ 2,000 Da), respectively. In comparison, F1 played a predominant role in the fouling behavior of the DNF effluent. Increased ozone dosage resulted in decreased membrane fouling contribution of F1 and increased fouling contribution of F2 and F3 during ozonation. The change of fouling contributions was attributed to the transformation of high MW fractions into lower MW fractions by ozonation. This study clarified the relationships between model parameters and the membrane fouling process caused by organic fractions with specific molecular weight, thus demonstrating the membrane fouling mechanism of the DNF effluent during ozonation.

Key words | correlation analysis, intermediate-standard model, membrane fouling mechanism, ozonation, redundancy analysis

Yuan Bai
Yin-Hu Wu (corresponding author)
Xin Tong
Yun-Hong Wang
Hong-Ying Hu IWA
Environmental Simulation and Pollution Control
   State Key Joint Laboratory, State Environmental
   Protection Key Laboratory of Microorganism
   Application and Risk Control (SMARC), School of
   Environment,
Tsinghua University,
Beijing 100084,
China
E-mail: *wuyinhu@mail.tsinghua.edu.cn*

Nozomu Ikuno
Kurita Water Industries Ltd.,
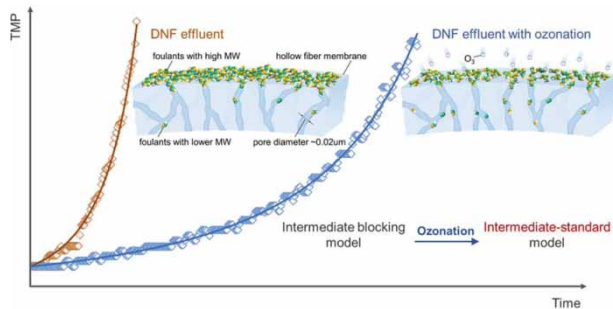Nakano-ku, Tokyo 164-0001,
Japan

Wei Wang
Yu-Long Shi
Beijing Drainage Group Company Limited,
Beijing,
China

Hong-Ying Hu
Shenzhen Environmental Science and New Energy
   Technology Engineering Laboratory,
Tsinghua-Berkeley Shenzhen Institute,
Shenzhen 518055,
China

HIGHLIGHTS

- Correlation between different MW fractions and model parameters was established.
- Fouling contribution of high and low MW fractions was assessed by model parameters.
- Change of model parameters illustrated conversion from high to low MW fractions.
- Intermediate blocking showed predominance over standard blocking during ozonation.
- Fouling control by ozonation could be quantitatively evaluated by model assessment.

GRAPHICAL ABSTRACT

INTRODUCTION

Nowadays, membrane filtration processes such as ultrafiltration (UF) have occupied a pivotal position of in-depth sewage treatment for water reclamation (Shen *et al.* 2012; Song *et al.* 2019). Membrane fouling continues to be one of the most significant problems working with UF (Guo *et al.* 2012; Yoo 2018). The investigation of the membrane fouling mechanism could contribute a great deal to solve the fouling problem and achieve stable operation of the system. Therefore, it is of great significance to identify and reveal the membrane fouling mechanism in the process of wastewater reclamation.

Membrane fouling is mainly related to pore blocking and the formation of the cake layer by deposition of foulants inside or on top of the membrane (Cerón-Vivas *et al.* 2018). Four prevailing mechanisms such as complete blocking, standard blocking, intermediate blocking and cake filtration have been adopted to describe membrane fouling (Ho & Zydney 2002; Iritani 2013). Complete blocking assumed that particles completely plugged membrane pores without superposition. In standard blocking, small particles deposited onto the internal pore walls of membrane, thus leading to a restriction of pore volume. Intermediate blocking was introduced by assuming that particles can settle on other deposited particles or membrane surface. Cake filtration occurred when particles accumulated on the membrane surface by forming a permeable cake of increasing thickness (Bowen *et al.* 1995; Suarez & Veza 2000).

The operation patterns of the UF membrane were based on constant-pressure mode (Aslam *et al.* 2015) and constant-flux mode (Kovalsky *et al.* 2009), the latter being more applied in most full-scale wastewater treatment systems (Kim & DiGiano 2009; Goldrick *et al.* 2017). Based on the filtration system with constant flux, fouling models derived from these four mechanisms have been developed to interpret the transmembrane pressure increase during operation (Hermia 1982; Hlavacek & Bouchet 1993). Table 1 summarizes the four fouling models with corresponding equations, which were related with the operating transmembrane pressure (P), initial transmembrane pressure (P_0), filtration time (t), initial flux (J_0) and the corresponding model parameters (K_b, K_s, K_i and K_c). On this basis, Bolton *et al.* (2006) proposed five new fouling models that accounted for the combined effects of the above-mentioned individual fouling mechanisms derived from Darcy's law. The combined models related to the same parameters (P, P_0, t and J_0) as individual models but considered simultaneously two of the model parameters (K_b, K_s, K_i and K_c) involved. Table 2 exhibits the equations of five combined fouling models for constant-flux operation.

Table 1 │ Equations of the individual fouling models for constant-flux operation

Model	Equation	Fitting parameter
Complete	$\dfrac{P}{P_0} = \dfrac{1}{1 - K_b t}$	K_b (s^{-1})
Standard	$\dfrac{P}{P_0} = \left(1 - \dfrac{K_s J_0 t}{2}\right)^{-2}$	K_s (m^{-1})
Intermediate	$\dfrac{P}{P_0} = e^{K_i J_0 t}$	K_i (m^{-1})
Cake	$\dfrac{P}{P_0} = 1 + K_c J_0^2 t$	K_c (s/m^2)

Table 2 | Equations of the combined fouling models for constant-flux operation

Model	Equation	Fitting parameters
Cake-complete	$\dfrac{P}{P_0} = \dfrac{1}{(1-K_b t)}\left(1 - \dfrac{K_c J_0^2}{K_b}\ln(1-K_b t)\right)$	K_c (s/m^2), K_b (s^{-1})
Cake-intermediate	$\dfrac{P}{P_0} = \exp(K_i J_0 t)\left(1 + \dfrac{K_c J_0}{K_i}(\exp(K_i J_0 t)-1)\right)$	K_c (s/m^2), K_i (m^{-1})
Complete-standard	$\dfrac{P}{P_0} = \dfrac{1}{(1-K_b t)\left(1 + \dfrac{K_s J_0}{2K_b}\ln(1-K_b t)\right)^2}$	K_b (s^{-1}), K_s (m^{-1})
Intermediate-standard	$\dfrac{P}{P_0} = \dfrac{\exp(K_i J_0 t)}{\left(1 - \dfrac{K_s}{2K_i}(\exp(K_i J_0 t)-1)\right)^2}$	K_i (m^{-1}), K_s (m^{-1})
Cake-standard	$\dfrac{P}{P_0} = \left(\left(1 - \dfrac{K_s J_0 t}{2}\right)^{-2} + K_c J_0^2 t\right)$	K_c (s/m^2), K_s (m^{-1})

Both individual and combined fouling models are widely applied to assess the blocking process of synthetic solutions, surface water or wastewater (Wang *et al.* 2018; Kirschner *et al.* 2019; Tong *et al.* 2020). Xing *et al.* (2019) applied fouling models to evaluate the fouling mitigation by UV and UV/chlorine oxidation, and standard pore blocking was proved to be crucial during the filtration process. Liu & Kim (2008) evaluated the performances of both blocking laws and artificial neural networks (ANNs) model, demonstrating that the combined cake-complete, cake-intermediate and ANNs models showed relative high consistency with experimental data. Liu *et al.* (2019) also used the fouling models on the ceramic membrane filtration for wastewater reclamation, reporting that the combined intermediate-standard model showed the best fit in all cases.

Due to the complexity of wastewater, researchers have revealed that the combined fouling models exhibited better fitting performances compared with single ones (Cerón-Vivas *et al.* 2018; Xiong *et al.* 2019; Li *et al.* 2020).

To illustrate the fouling process, models were proposed with idealized particles and membrane pores based on theoretical assumptions. But in practical engineering, the fouling phenomena caused by wastewater were rather complex and closely related to various water features, such as viscosity, hydrophobicity and molecular weight (MW) distribution (Kang *et al.* 2011; Shen *et al.* 2012). Therefore, to further demonstrate the influence of water features on membrane fouling, it is of importance to analyze the model assessment results based on water features. This is

of great practical significance to clarify the membrane fouling mechanism and propose fouling control strategies. However, related researches are rarely reported.

In this study, we compared the fitting performances of different models in the fouling process of the denitrification filter (DNF) effluent during ozonation. Furthermore, correlation analysis and redundancy analysis (RDA) were conducted to investigate the correlations among the model parameters, fouling potential and water features of the DNF effluent, thus endowing the model parameters with practical significance in our system. Based on the fitting results at different ozone dosages, the quantitative relationships among ozone dosage, water features and fouling potential were established. The membrane fouling mechanism of the DNF effluent during ozonation was revealed and this study helped glean valuable insight into membrane fouling control by model assessment in the UF system.

MATERIALS AND METHODS

Ozonation and membrane fouling experiments

Feed water of this study was the DNF effluent collected from the wastewater reclamation plant of Gaobeidian, Beijing. The feed water was transported to the laboratory immediately after sampling for experiments. The major water characteristics including DOC (dissolved organic carbon), COD (chemical oxygen demand), SS (suspended solids),

TN (total nitrogen), pH, and turbidity of the feed sample are listed in Supplementary Material, Table S1.

Ozonation experiments were conducted using a stock solution with maximum ozone concentration of 40 mg/L prepared by an ozone generator (CF-YG20, Shanmeishuimei High Technology Co., Ltd). The volumes of the original DNF effluent and the stock solution of water samples with different ozone dosages were calculated firstly before ozonation, and the final DOC concentration of each sample was set at 4 mg/L. After ozonation treatment, the DOC of each water sample was almost unchanged and no residual ozone could be detected after 6-min storage.

The filtration experiments were conducted under the constant flux of 180 L/m^2 h using a dead-end filtration system as shown in Supplementary Material, Figure S1, which was described in detail in our previous work (Bai *et al.* 2020). The membrane module was constructed with a single hollow fiber membrane (PVDF) with a nominal pore diameter of 0.02 μm. A constant flow pump was set to maintain the working flux. The threshold transmembrane pressure (TMP) was fixed at 3 bar, and the pump would be stopped at once when the TMP reached the fixed value. An electronic balance was used to monitor the flow rate, while a pressure sensor was used to monitor the TMP change during the filtration process in real time. Each filtration experiment in this study has been repeated three times.

Water feature characterization

The DOC concentration, fluorescence excitation emission matrix spectra and UV$_{254}$ value of water samples were determined by a total organic carbon (TOC) analyzer (TOC-VCPH, SHIMADZU), a fluorescence spectrophotometer (F-7000, Hitachi) and a UV–Vis spectrophotometer (UV-2450, Shimadzu, Japan), respectively. A rapid digested spectrophotometry method (HJ/T 399-2007) was used to determine COD concentration. A pH meter (Seven2Go, Mettler Toledo, Switzerland) was used to measure the pH value. Chinese States Standard Testing Methods (State Environmental Protection Administration 2002) were used to measure TN. The apparent MW distribution was determined following the reported method (Wang *et al.* 2017) by a high-performance size-exclusion chromatography (HPSEC; LC20-AD, Shimadzu, Japan). The mobile phase, which was composed of

2.4 mM KH$_2$PO$_4$, 3.6 mM K$_2$HPO$_4$ and 25 mM Na$_2$SO$_4$, was injected of 100 μL with a flow rate of 0.5 mL/min. Water samples were filtered by a 0.45 μm membrane, and the filtrates were used for the above-mentioned analyses.

The filtration and analytical results of water samples with ozonation treatment were reported by the authors' previous study. For more detailed information, refer to Bai *et al.* (2020).

Modeling analysis of the membrane fouling process

In this study, to further investigate the membrane fouling mechanism of DNF effluent during ozonation, five fouling models including four individual models and one combined model (intermediate-standard model) in Tables 1 and 2 were applied to fit the experimental data in ORIGIN. The fitting results of models were evaluated based on the sum of squares of residuals (SSR) and the determination coefficient (R^2).

Statistical analysis of the membrane fouling process

A method of RDA was adopted to determine the correlations among the model parameters, fouling potential and water features of the DNF effluent during ozonation with different ozone dosages (0–2 mg O$_3$/mg C). The water features of membrane influent, including DOC, UV$_{254}$, EEM, F1, F2 and F3, were set as six explanatory variables. EEM represented the fluorescence intensity of excitation emission matrix spectra. F1, F2 and F3 represented the proportion of high (>4,000 Da), medium (2,000–4,000 Da) and low (<2,000 Da) apparent MW fractions, respectively. Model parameters K_i and K_s of the combined intermediate-standard model and the filtration time t for the TMP reaching 3 bar were set as three different response variables. All explanatory and response variables consisted of the results of three repeated experiments. Logarithmic transformation was performed on the raw data of all response variables and the significance of the explanatory variables for response variables was evaluated by 499 times of Monte-Carlo permutation test. RDA analysis was performed with CANOCO version 5.0 (Microcomputer Power, USA) according to published methods (ter Braak & Smilauer 2012).

To assess the correlations among the model parameters, fouling potential and water features of the DNF effluent at different conditions of ozonation (0–2 mg O$_3$/mg C), IBM

SPSS Statistics version 25.0 was applied in the correlation analysis of the data.

RESULTS AND DISCUSSION

Filtration tests of DNF effluent with ozonation treatment

Filtration tests of DNF effluent with ozonation is shown in Figure 1. The control sample without ozonation showed the fastest fouling rate with the filtration time of 80 min for the TMP increased to 3 bar. However, effective membrane fouling alleviation was achieved after ozonation treatment, and the alleviation performance was more significant as increased O_3 dosage. Compared with the original DNF effluent, the filtration time was prolonged by 1.125, 1.6, 2, 2.65 and 3.75 times with O_3 dosage of 0.1, 0.25, 1, 1.5 and 2 mg O_3/mg C, respectively. These results demonstrated the effective alleviation performance of membrane fouling by ozonation. The data of filtration tests were reported in the authors' previous study (Bai *et al.* 2020).

Modeling analysis of the membrane fouling process caused by the DNF effluent during ozonation
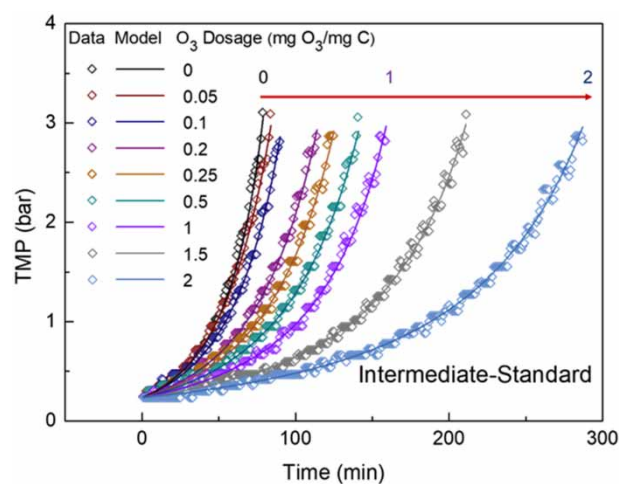
In order to acquire an explicit and profound understanding of the membrane fouling mechanism from the perspective of modeling analysis, four widely applied individual fouling models mentioned above (Table 1) were applied to interpret the experimental data of DNF effluent during ozonation. Figure 1 compares the fitting results of water samples treated with different ozone dosages for each model, and the model parameters (K_b, K_s, K_i and K_c), SSR and R^2 of each run are shown in Supplementary Material, Table S2. The fitting results of the cake or complete fouling model were not
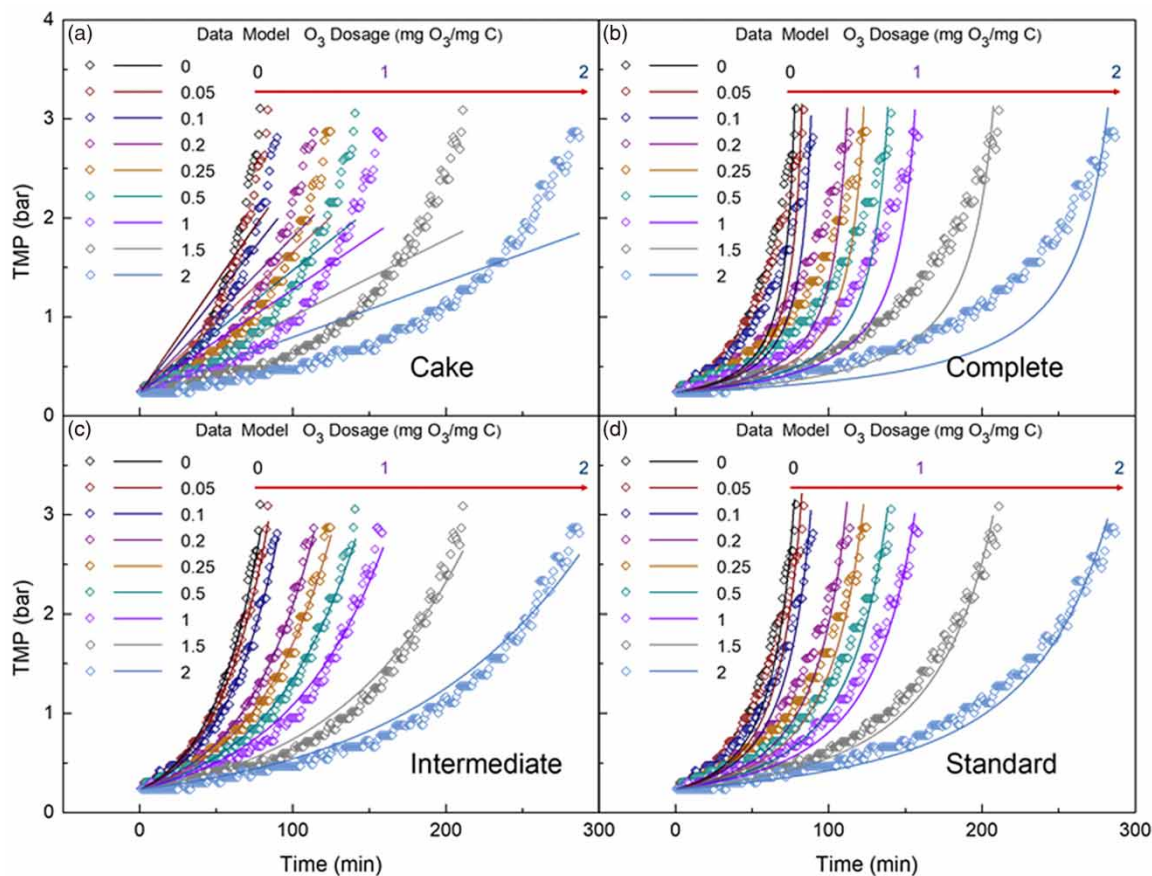
Figure 1 | Prediction of membrane fouling using the individual (a) cake, (b) complete, (c) intermediate and (d) standard model for experimental data.

promising with much lower R^2 and higher SSR values, while the standard fouling model exhibited improved fitting results especially at higher ozone dosages. Among the four applied models, the intermediate fouling model presented the best-fit performance at all ozone dosages. But the fitting performance became less satisfactory with increased ozone dosage. According to the results in Supplementary Material, Table S2, relatively low R^2 and high SSR were obtained at high ozone dosage, suggesting marked deviation between the intermediate model and experimental results after high-dosage ozonation. These results indicated that an individual fouling model was insufficient to elucidate the membrane fouling mechanism of the DNF effluent during ozonation, since several blocking laws might contribute simultaneously to the membrane fouling process (Liu & Kim 2008).

According to the fitting results of the forementioned models, we seek to analyze the data by applying the combined fouling models based on the intermediate model. Considering the improved fitting performance of the standard model at high ozone dosages, the combined intermediate-standard model was applied to describe the filtration process (Figure 2), and the specific fitting results are shown in Table 3. The combined model showed more precise fitting performance than the forementioned individual models, with all R^2 larger than 0.99 at different ozone dosages. According to these results, we speculated that the membrane fouling behavior in our study was more likely attributed to the combination of intermediate and standard blocking laws.
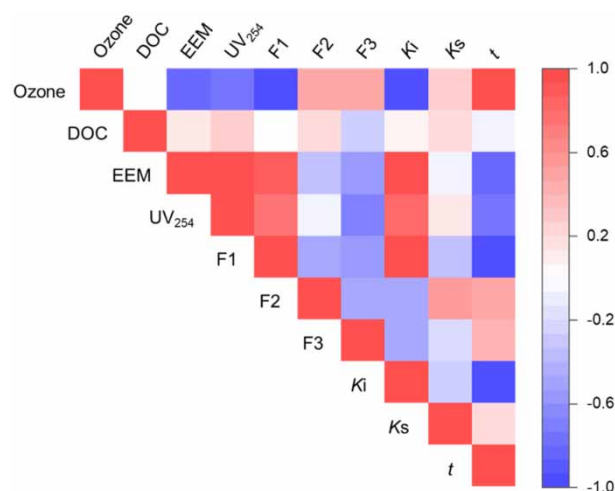
Table 3 | Fitting parameters of each run with the combined intermediate-standard model

| | | Intermediate-standard | | | |
Ozone dosage (mg O_3/mg C)	K_i (m^{-1})	K_s (m^{-1})	K_i/K_s	R^2	SSR
0	9.40	0.39	24.10	0.996	0.19
0.05	9.63	0.15	64.20	0.992	0.40
0.1	8.58	0.20	42.90	0.996	0.19
0.2	6.92	0.14	49.43	0.996	0.23
0.25	6.16	0.17	36.24	0.995	0.34
0.5	5.27	0.20	26.35	0.995	0.33
1	3.99	0.31	12.87	0.995	0.43
1.5	2.80	0.39	7.18	0.995	0.48
2	2.01	0.41	4.91	0.995	0.63

Correlations among the model parameters, fouling potential and water features of the DNF effluent

In order to further explore the influence of water features on membrane fouling and seek out the practical significance of the model parameters, correlation analysis was applied to quantify the correlations among the model parameters, fouling potential and water features of the DNF effluent (Figure 3 and Supplementary Material, Table S3). The filtration time t before the operational pressure reached 3 bar, which was the direct indicator of membrane fouling potential, had markedly negative correlation with K_i (fitting parameter of

Figure 2 | Prediction of membrane fouling using the combined intermediate-standard model for experimental data.

Figure 3 | Correlations among the model parameters, fouling potential and water features of the DNF effluent. EEM represented the fluorescence intensity of excitation emission matrix spectra. F1, F2 and F3 represented the proportion of high (>4,000 Da), medium (2,000–4,000 Da) and low (<2,000 Da) apparent molecular weight fractions, respectively.

intermediate blocking in intermediate-standard model), indicating that intermediate blocking played a crucial role on membrane fouling and larger K_i corresponded to higher fouling potential. By contrast, the filtration time t presented the indistinctive positive correlation with K_s (fitting parameter of standard blocking in intermediate-standard model), suggesting that standard blocking showed a minor influence on membrane fouling. Therefore, intermediate blocking had a greater predominance over standard blocking in the fouling mechanism of the DNF effluent.

Reduction of organic load and structural changes of organic matters were two common explanations for membrane fouling control by ozonation (Van Geluwe *et al.* 2011; Wei *et al.* 2016). In this study, the correlations of DOC concentration with K_i and K_s were quite low, suggesting that it was structural changes of organic matters rather than the DOC concentration that played predominant roles on membrane fouling during ozonation. As for the other water features, K_i showed the highest positive correlation (0.95) with F1 (the proportion of organic fractions >4,000 Da) but a negative correlation with F2 (the proportion of organic fractions 2,000–4,000 Da) and F3 (the proportion of organic fractions <2,000 Da). By contrast, opposite correlations of K_s with F1, F2 and F3 were obtained. EEM and UV_{254} were also positively correlated with K_i, which might be attributed to their positive correlationships with F1. These results demonstrated that K_i (corresponding to intermediate blocking) was fairly applicable to describe membrane fouling caused by high MW fractions (F1) of the DNF effluent. While K_s (corresponding to standard blocking) was more suitable to represent the membrane fouling caused by lower MW fractions (F2 and F3).

In terms of the specific hypothesis of fouling models, intermediate blocking law presumes that the mean particle size (d_p) was larger than the average pore diameter (D_p), while d_p was presumed to be smaller than D_p in standard blocking law (Sabia *et al.* 2016; Ochando-Pulido & Martínez-Ferez 2017). In other words, intermediate and standard blocking laws were widely used to describe the membrane fouling process by large and small particles, respectively. Our analytical results were in accordance with the theoretical assumptions and further established the correlation between the model parameters and water features of the DNF effluent, endowing K_i and K_s with a practical significance in our system.

RDA was carried out to comprehensively analyze the quantitative relationships among the model parameters, fouling potential and water features of the DNF effluent (Figure 4). In the RDA diagram, the angle between any two vectors represents the correlation between them (the smaller the angle, the greater the correlation). The Axis 1 and Axis 2 of RDA explained 92.7 and 3.9% of the variance, respectively. Therefore, Axis 1 could largely reflect the degree of membrane fouling. The correlation analytical results were in accordance with Figure 3. Moreover, F1 was the most important factor and could account for nearly 90% of the membrane fouling caused by the DNF effluent, which was significant at the level of 0.002. It further confirmed that the fouling of F1 corresponding to the intermediate blocking played a predominant role in membrane fouling of the DNF effluent.

Quantitative analysis of the ozonation influence on membrane fouling by model assessment

Based on RDA results, the experimental data could be classified into three groups (Figure 4). The first group was represented by the control sample without ozonation, and the data points were plotted at the top of the graph. The second group included the water samples treated by lower ozone dosages (0.05, 0.1, 0.2, 0.25 and 0.5 mg O_3/mg C) with data points plotted at the bottom left of the graph. The third group consisted of the water samples treated by
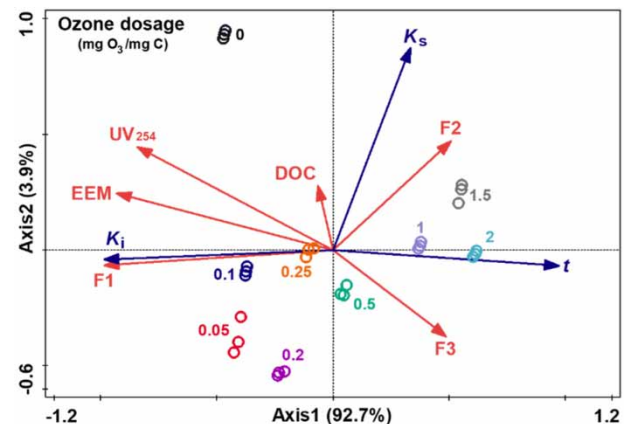
Figure 4 | Redundancy analysis (RDA) of the relationships among the model parameters, fouling potential and water features of the DNF effluent. EEM represented the fluorescence intensity of excitation emission matrix spectra. F1, F2 and F3 represented the proportion of high (>4,000 Da), medium (2,000–4,000 Da) and low (<2,000 Da) apparent molecular weight fractions, respectively.

high ozone dosages (1, 1.5 and 2 mg O_3/mg C) with data points plotted at right of the graph. The grouping results demonstrated that ozonation treatment had significant impacts on water features of the DNF effluent, resulting in the diverse fouling potential of water samples after ozonation. In addition, ozonation showed relatively higher correlations with all water features (Figure 3), suggesting the marked influence of ozonation on water features as well.

Table 3 exhibits the quantitative variations of fouling parameters in the combined intermediate-standard model during ozonation. Increased ozone dosage led to decreased K_i and increased K_s, corresponding to decreased membrane fouling caused by high MW fractions and increased fouling caused by lower MW fractions during ozonation, respectively. The respective contribution of the two individual blocking laws can be evaluated from the magnitudes of the fitting parameters (Cerón-Vivas *et al.* 2018). Decreased K_i/K_s (Table 3) during ozonation suggested the decreased contribution of intermediate blocking and increased contribution of standard blocking, which was in accordance with the fitting performances in Figure 1(c) and 1(d). The change of fouling contributions corresponded to the transformation process of high MW fractions into lower MW fractions by ozonation (Figure 5). As for the DNF effluent, high MW fractions accounted for the major part of the organic foulants and thus intermediate blocking played as a critical fouling mechanism (Figure 5(a)). After ozonation
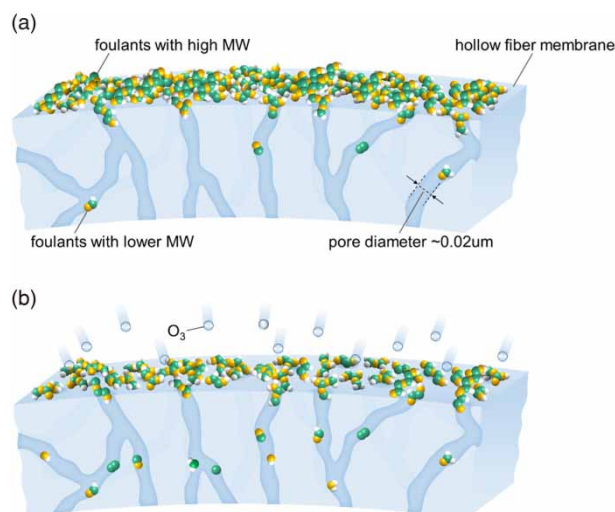
treatment, the proportion of high MW fractions decreased and that of lower MW fractions increased, and thus standard blocking need to be taken into consideration to clarify the overall fouling process (Figure 5(b)).

However, K_i was about one or two magnitudes larger than K_s at all ozone dosages, indicating greater contribution of intermediate blocking in membrane fouling. This was in accordance with the RDA results in the section 'Correlations among the model parameters, fouling potential and water features of the DNF effluent' that the intermediate blocking mechanism played a predominant role over standard blocking under our experimental conditions in spite of the inverse contribution changes of the two blocking laws after ozonation. Therefore, remarkable fouling alleviation achieved by ozonation was actually ascribed to the alleviation of intermediate blocking by the transformation of high MW fractions into lower MW fractions. Studies have also reported that ozonation could achieve significant membrane fouling alleviation by degradation of higher MW fractions (Zhu *et al.* 2010; Tang *et al.* 2017; Jin *et al.* 2019; Zhao *et al.* 2019).

In order to further describe the change of model parameters during ozonation, the Michaelis–Menten equation was modified and adopted (Equation (1)) in this study and the results are shown in Figure 6:

$$K_i = K_{i\,max} - \frac{K_{i\,max}[O_3]}{A_m + [O_3]}, \quad Ks = \frac{K_{s\,max}[O_3]}{B_m + [O_3]} \tag{1}$$

$[O_3]$ represents the concentration of ozone, $K_{i\,max}$ and $K_{s\,max}$ represent the theoretical maximal value of K_i and K_s, respectively. A_m represents the ozone concentration when K_i equals to $1/2K_{i\,max}$ and B_m represents the ozone concentration when K_s equals to $1/2K_{s\,max}$.
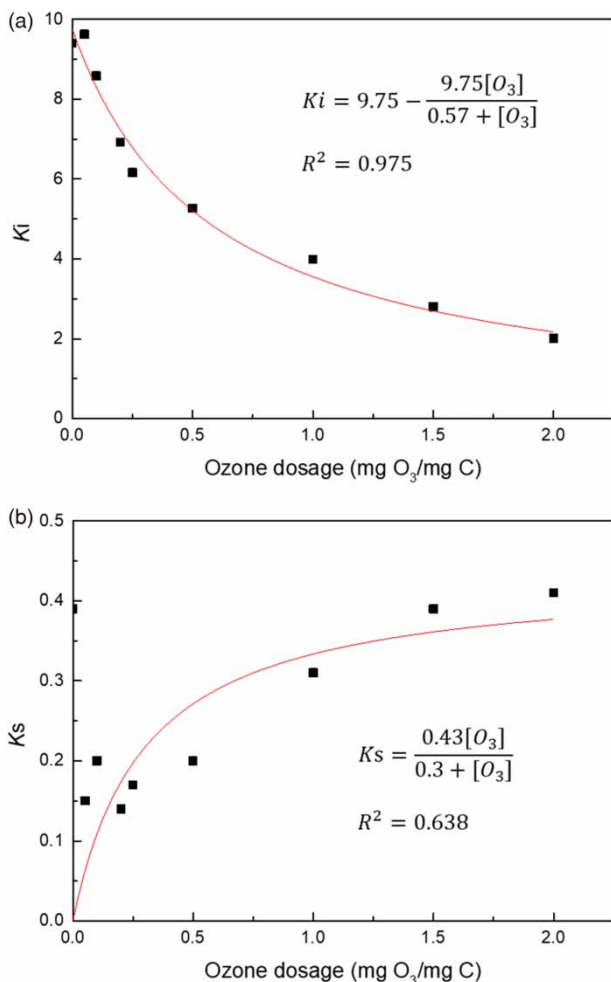
The fitting results of the modified Michaelis–Menten equation are shown in Equation (2):

$$K_i = 9.75 - \frac{9.75[O_3]}{0.57 + [O_3]}, \quad R^2 = 0.975$$

$$K_s = \frac{0.43[O_3]}{0.3 + [O_3]}, \quad R^2 = 0.638 \tag{2}$$

Specifically, K_i decreased significantly and showed good fit with ozone dosage ($R^2 = 0.975$). These results further implied that the change of K_i during ozonation could be

Figure 5 | Schematic diagrams of the membrane fouling process caused by the DNF effluent (a) before and (b) after ozonation treatment.

$$Ki = 9.75 - \frac{9.75[O_3]}{0.57 + [O_3]}$$

$$R^2 = 0.975$$

$$Ks = \frac{0.43[O_3]}{0.3 + [O_3]}$$

$$R^2 = 0.638$$

Figure 6 | Model parameters (a) K_i and (b) K_s of the combined intermediate-standard model as a function of ozone dosage.

quantitatively evaluated as a function of ozone dosage. In practical engineering, the membrane fouling control performance by ozonation, especially the degradation efficiency of high MW fractions, could be predicted by quantitative evaluation via the change of K_i by model assessment.

CONCLUSIONS

- The combined intermediate-standard model was promising to evaluate the fouling process of the DNF effluent during ozonation.
- Model parameter K_i corresponding to intermediate blocking was fairly applicable to describe the fouling caused by high MW fractions (F1, MW > 4,000 Da),

while K_s corresponding to standard blocking was more suitable to describe the fouling caused by lower MW fractions (F2, MW = 2,000–4,000 Da and F3, MW < 2,000 Da) of the DNF effluent in this study.

- During ozonation, increased ozone dosage led to decreased K_i and increased K_s, indicating decreased fouling contribution of high MW fractions and increased fouling contribution of lower MW fractions, respectively.
- Intermediate blocking mechanism played a predominant role over standard blocking under the experimental conditions of this study. RDA results revealed that F1 was the most important factor to affect membrane fouling of the DNF effluent, accounting for nearly 90% of the fouling variation ($p = 0.002$).
- In practical engineering, model parameters were closely correlated with water features and the fouling control performance by ozonation could be quantitatively evaluated via the change of model parameters.

ACKNOWLEDGEMENTS

CONFLICT OF INTEREST

The authors declare no financial or commercial conflicts of interest.

DATA AVAILABILITY STATEMENT

All relevant data are included in the paper or its Supplementary Information.

REFERENCES

Aslam, M., Lee, P.-H. & Kim, J. 2015 Analysis of membrane fouling with porous membrane filters by microbial suspensions for

autotrophic nitrogen transformations. *Sep. Purif. Technol.* **146**, 284–293.

Bai, Y., Wu, Y.-H., Wang, Y.-H., Tong, X., Zhao, X.-H., Ikuno, N. & Hu, H.-Y. 2020 Membrane fouling potential of the denitrification filter effluent and the control mechanism by ozonation in the process of wastewater reclamation. *Water Res.* **173**, 115591.

Bolton, G., LaCasse, D. & Kuriyel, R. 2006 Combined models of membrane fouling: development and application to microfiltration and ultrafiltration of biological fluids. *J. Membr. Sci.* **277** (1), 75–84.

Bowen, W. R., Calvo, J. I. & Hernández, A. 1995 Steps of membrane blocking in flux decline during protein microfiltration. *J. Membr. Sci.* **101** (1), 153–165.

Cerón-Vivas, A., Kalboussi, N., Morgan-Sagastume, J. M., Harmand, J. & Noyola, A. 2018 Model assessment of the prevailing fouling mechanisms in a submerged membrane anaerobic reactor treating low-strength wastewater. *Bioresour. Technol.* **268**, 460–469.

Goldrick, S., Joseph, A., Mollet, M., Turner, R., Gruber, D., Farid, S. S. & Titchener-Hooker, N. J. 2017 Predicting performance of constant flow depth filtration using constant pressure filtration data. *J. Membr. Sci.* **531**, 138–147.

Guo, W., Ngo, H.-H. & Li, J. 2012 A mini-review on membrane fouling. *Bioresour. Technol.* **122**, 27–34.

Hermia, J. 1982 Constant pressure blocking filtration laws-application to power-law non-Newtonian fluids. *Trans. Inst. Chem. Eng.* **60** (3), 183–187.

Hlavacek, M. & Bouchet, F. 1993 Constant flowrate blocking laws and an example of their application to dead-end microfiltration of protein solutions. *J. Membr. Sci.* **82** (3), 285–295.

Ho, C. C. & Zydney, A. L. 2002 Transmembrane pressure profiles during constant flux. Microfiltration of bovine serum albumin. *J. Membr. Sci.* **209** (2), 363–377.

Iritani, E. 2013 A review on modeling of pore-blocking behaviors of membranes during pressurized membrane filtration. *Drying Technol.* **31** (2), 146–162.

Jin, X., Zhang, W., Hou, R., Jin, P., Song, J. & wang, X. C. 2019 Tracking the reactivity of ozonation towards effluent organic matters from WWTP using two-dimensional correlation spectra. *J. Environ. Sci.* **76**, 289–298.

Kang, X., Wang, X., Xia, H., Waite, T. D. & Wen, X. 2011 Combined effect of membrane and foulant hydrophobicity and surface charge on adsorptive fouling during microfiltration. *J. Membr. Sci.* **373** (1–2), 140–151.

Kim, J. & DiGiano, F. A. 2009 Fouling models for low-pressure membrane systems. *Sep. Purif. Technol.* **68** (3), 293–304.

Kirschner, A. Y., Cheng, Y.-H., Paul, D. R., Field, R. W. & Freeman, B. D. 2019 Fouling mechanisms in constant flux crossflow ultrafiltration. *J. Membr. Sci.* **574**, 65–75.

Kovalsky, P., Bushell, G. & Waite, T. D. 2009 Prediction of transmembrane pressure build-up in constant flux microfiltration of compressible materials in the absence and presence of shear. *J. Membr. Sci.* **344** (1), 204–210.

Li, R., Gao, B., Wang, W., Yue, Q. & Wang, Y. 2020 Floc properties and membrane fouling in coagulation/ultrafiltration process for the treatment of Xiaoqing River: the role of polymeric aluminum-polymer dual-coagulants. *Chemosphere* **243**, 125391.

Liu, Q.-F. & Kim, S.-H. 2008 Evaluation of membrane fouling models based on bench-scale experiments: a comparison between constant flowrate blocking laws and artificial neural network (ANNs) model. *J. Membr. Sci.* **310** (1), 393–401.

Liu, J., He, K., Zhang, J., Li, C. & Zhang, Z. 2019 Coupling ferrate pretreatment and in-situ ozonation/ceramic membrane filtration for wastewater reclamation: water quality and membrane fouling. *J. Membr. Sci.* **590**, 117310.

Ochando-Pulido, J. M. & Martínez-Ferez, A. 2017 Fouling modelling on a reverse osmosis membrane in the purification of pretreated olive mill wastewater by adapted crossflow blocking mechanisms. *J. Membr. Sci.* **544**, 108–118.

Sabia, G., Ferraris, M. & Spagni, A. 2016 Model-based analysis of the effect of different operating conditions on fouling mechanisms in a membrane bioreactor. *Environ. Sci. Pollu. Res.* **23**, 1598–1609.

Shen, Y.-x., Xiao, K., Liang, P., Sun, J.-y., Sai, S.-j. & Huang, X. 2012 Characterization of soluble microbial products in 10 large-scale membrane bioreactors for municipal wastewater treatment in China. *J. Membr. Sci.* **415–416**, 336–345.

Song, Y., Hu, Q., Sun, Y., Li, X., Wan, H., Zang, L., Jiang, K. & Gao, C. 2019 The feasibility of UF-RO integrated membrane system combined with coagulation/flocculation for hairwork dyeing effluent reclamation. *Sci. Total Environ.* **691**, 45–54.

State Environmental Protection Administration 2002 *Monitoring Method of Water and Wastewater*. 4th edn. China Environmental Science Press, Beijing, 105, pp. 246–248, 255–257.

Suarez, J. A. & Veza, J. M. 2000 Dead-end microfiltration as advanced treatment for wastewater. *Desalination* **127** (1), 47–58.

Tang, S., Zhang, Z. & Zhang, X. 2017 New insight into the effect of mixed liquor properties changed by pre-ozonation on ceramic UF membrane fouling in wastewater treatment. *Chem. Eng. J.* **314**, 670–680.

ter Braak, C. J. F. & Smilauer, P. 2012 *Canoco Reference Manual and User's Guide: Software for Ordination, Version 5.0.* Microcomputer Power, Ithaca, New York.

Tong, X., Wu, Y.-H., Wang, Y.-H., Bai, Y., Zhao, X.-H., Luo, L.-W., Mao, Y., Ikuno, N. & Hu, H.-Y. 2020 Simulating and predicting the flux change of reverse osmosis membranes over time during wastewater reclamation caused by organic fouling. *Environ. Int.* **140**, 105744.

Van Geluwe, S., Braeken, L. & Van der Bruggen, B. 2011 Ozone oxidation for the alleviation of membrane fouling by natural organic matter: a review. *Water Res.* **45** (12), 3551–3570.

Wang, W.-L., Zhang, X., Wu, Q.-Y., Du, Y. & Hu, H.-Y. 2017 Degradation of natural organic matter by UV/chlorine oxidation: molecular decomposition, formation of oxidation byproducts and cytotoxicity. *Water Res.* **124**, 251–258.

Wang, L., Liu, H., Zhang, W., Yu, T., Jin, Q., Fu, B. & Liu, H. 2018 Recovery of organic matters in wastewater by self-forming dynamic membrane bioreactor: performance and membrane fouling. *Chemosphere* **203**, 123–131.

Wei, D., Tao, Y., Zhang, Z. & Zhang, X. 2016 Effect of pre-ozonation on mitigation of ceramic UF membrane fouling caused by algal extracellular organic matters. *Chem. Eng. J.* **294**, 157–166.

Xing, J., Liang, H., Xu, S., Chuah, C. J., Luo, X., Wang, T., Wang, J., Li, G. & Snyder, S. A. 2019 Organic matter removal and membrane fouling mitigation during algae-rich surface water treatment by powdered activated carbon adsorption pretreatment: enhanced by UV and UV/chlorine oxidation. *Water Res.* **159**, 283–293.

Xiong, J., Zuo, X., Zhang, S., Liao, W. & Chen, Z. 2019 Model-based evaluation of fouling mechanisms in powdered activated carbon/membrane bioreactor system. *Water Sci. Technol.* **79** (10), 1844–1852.

Yoo, S. S. 2018 Operating cost reduction of in-line coagulation/ultrafiltration membrane process attributed to coagulation condition optimization for irreversible fouling control. *Water* **10** (8), 1076–1093.

Zhao, X., Wu, Y., Zhang, X., Tong, X., Yu, T., Wang, Y., Ikuno, N., Ishii, K. & Hu, H. 2019 Ozonation as an efficient pretreatment method to alleviate reverse osmosis membrane fouling caused by complexes of humic acid and calcium ion. *Front. Environ. Sci. Eng.* **13** (4), 55–67.

Zhu, H., Wen, X. & Xia, H. 2010 Membrane organic fouling and the effect of pre-ozonation in microfiltration of secondary effluent organic matter. *J. Membr. Sci.* **352** (1–2), 213–221.